Original Article

http://dx.doi.org/10.3349/ymj.2012.53.6.1147
pISSN: 0513-5796, eISSN: 1976-2437

Yonsei Med J 53(6):1147-1153, 2012

YMJ

# Quantitative Assessment of Tumor Responses after Radiation Therapy in a DLD-1 Colon Cancer Mouse Model Using Serial Dynamic Contrast-Enhanced Magnetic Resonance Imaging

Sung Jun Ahn,[1] Woong Sub Koom,[2] Chan Sik An,[1] Joon Seok Lim,[1] Seung-Koo Lee,[1] Jin-Suck Suh,[1] and Ho-Taek Song[1]

[1]Department of Radiology and Research Institute of Radiological Science, [2]Department of Radiation Oncology, Yonsei University College of Medicine, Seoul, Korea.

Received: October 6, 2011
Revised: December 8, 2011
Accepted: December 9, 2011
Corresponding author: Dr. Ho-Taek Song, Department of Radiology, Yonsei University College of Medicine, 50 Yonsei-ro, Seodaemun-gu, Seoul 120-752, Korea.
Tel: 82-2-2228-2370, Fax: 82-2-393-3035
E-mail: hotsong@yuhs.ac

· The authors have no financial conflicts of interest.

**Purpose:** The purpose of this study was to investigate the predictability of pretreatment values including Dynamic Contrast-Enhanced Magnetic Resonance Imaging (DCE-MRI) derived parameters ($K^{trans}$, $K_{ep}$ and $V_e$), early changes in parameters ($K^{trans}$, tumor volume), and heterogeneity (standard deviation of $K^{trans}$) for radiation therapy responses via a human colorectal cancer xenograft model. **Materials and Methods:** A human colorectal cancer xenograft model with DLD-1 cancer cells was produced in the right hind limbs of five mice. Tumors were irradiated with 3 fractions of 3 Gy each for 3 weeks. Baseline and follow up DCE-MRI were performed. Quantitative parameters ($K^{trans}$, $K_{ep}$ and $V_e$) were calculated based on the Tofts model. Early changes in $K^{trans}$, standard deviation (SD) of $K^{trans}$, and tumor volume were also calculated. Tumor responses were evaluated based on histology. With a cut-off value of 0.4 for necrotic factor, a comparison between good and poor responses was conducted. **Results:** The good response group (mice #1 and 2) exhibited higher pretreatment $K^{trans}$ than the poor response group (mice #3, 4, and 5). The good response group tended to show lower pretreatment $K_{ep}$, higher pretreatment $V_e$, and larger baseline tumor volume than the poor response group. All the mice in the good response group demonstrated marked reductions in $K^{trans}$ and SD value after the first radiation. All tumors showed increased volume after the first radiation therapy. **Conclusion:** The good response after radiation therapy group in the DLD-1 colon cancer xenograft nude mouse model exhibited a higher pretreatment $K^{trans}$ and showed an early reduction in $K^{trans}$, demonstrating a more homogenous distribution.

**Key Words:** Colorectal cancer, radiation therapy, magnetic resonance imaging, permeability, angiogenesis



## INTRODUCTION

Colorectal cancer is a frequently diagnosed cancer with high mortality. In patients

with advanced stage, preoperative radiation therapy or preoperative concurrent chemo-radiation therapy (CCRT) is frequently administered.[1-3] Such therapies are useful for decreasing rates of recurrence.[4] However, there are currently no methods for predicting which tumors will respond to radiation therapy.

Tumor vascularity and oxygenation status have long been advocated as important factors that influence tumor responses to radiation therapy.[5] Dynamic contrast-enhanced magnetic resonance imaging (DCE-MRI) combined with pharmacokinetic modeling has emerged as a promising noninvasive imaging technique for evaluating tumor microvasculature, generating quantitative parameters of microcirculation based on the two-compartment Tofts model.[6,7] According to this model, contrast enters the intravascular space (compartment 1), passes into the interstitial space (compartment 2), and reenters the intravascular space (compartment 1). During this course, $K^{trans}$ represents the rate of which the contrast media passes from the intravascular space to the interstitial space. $K_{ep}$ signifies the rate constant for back diffusion of the contrast agent from the interstitial space into the intravascular space. $V_e$ denotes extravascular-extracellular leakage space. Several studies have shown that DCE-MRI derived parameters are related to tumor responses to treatment. George, et al.[8] showed that responsive tumors had higher pretreatment $K^{trans}$ values than non-responsive tumors in colorectal cancer. In addition, Ah-See, et al.[9] recently reported that early changes in $K^{trans}$ are the best predictor for treatment responses to chemotherapy in patients with breast cancer. Meanwhile, Yu, et al.[10] showed that early changes in tumor size are better response predictors than other DCE derived parameters. Furthermore, some studies emphasized the analysis of intratumoral heterogeneity. According to one study, standard deviation (SD) of pixel values for $K^{trans}$ could allow for improved diagnostic accuracy for distinguishing breast cancer from benign lesions.[11] Accordingly, a response group treated for locally advanced breast cancer exhibited significant reductions in SD of enhancement amplitude, demonstrating a more homogenous distribution after treatment.[12] Although the results of several reports have been published, the predictability of DCE-derived parameters are still debated and not standardized.

The aim of this study was to investigate the predictability of pretreatment values including DCE-MRI derived parameters ($K^{trans}$, $K_{ep}$ and $V_e$), early changes in parameters ($K^{trans}$, tumor volume), and heterogeneity (standard deviation of $K^{trans}$) for radiation therapy responses via a human colorectal cancer xenograft model.

## MATERIALS AND METHODS

### Experimental model

All experiments followed institutional guidelines for the care and use of laboratory animals. A human DLD-1 colon cancer cell suspension ($1\times10^6$ cells in 100 μL of phosphate buffered saline) was implanted subcutaneously into the right hind limbs of five 5-week-old (SLC, Kotoh-cho, Japan) female nude mouse. Tumors were allowed to grow for approximately 7 to 14 days, until reaching an approximate longest diameter of 1 cm before initiating radiation therapy. However, there was some degree of variability in volume because the tumors in each mouse did not grow at exactly the same rate.

### Irradiations

The mice were anesthetized by intraperitoneal injection of a mixture of Zoletil (40 mg/kg) and Rompun (5 mg/kg) to achieve reproducible prone positioning during treatment. Irradiations were performed with a linear accelerator (CGR, Paris, France) using a beam of 18-MV photons. The dose rate was 200 cGy/min at a focus-to-skin distance of 127 cm. The hind leg subcutaneously implanted tumor was irradiated while the remainder of the mouse was shielded with 8-cm-thick Arplay Cerro (Arplay, Izeure, France), positioned on top of a 2.5-cm Plexiglas™ (Rohm and Haas company, Philadelphia, PA, USA) plate necessary for electronic equilibrium. Dosimetry in the treatment position was performed using LiF pastilles positioned at the area of tumor cell inoculation to indicate accurate dose delivery to the tumor. Each mouse received 3 fractions of 3 Gy each for a total of 21 days at an interval of 7 days. After three cycles of irradiations were completed, the nude mice were euthanized.

### MR examinations

DCE MRI was performed four times for each mouse. The first base line study was performed immediately before initiating radiation therapy. The other three MRIs were performed one week after each radiation therapy.

Magnetic resonance imaging was performed using a whole-body 3T MR scanner (MAGNETOM Tim Trio, Siemens Healthcare, Erlangen, Germany) and a four-phased array wrist coil (Siemens Healthcare). The mice were placed

prone in a plastic holder and connected to a mask carrying inhaled anesthetic to restrict movement. The mice were initially anesthetized with 4% isoflurane inhalation, and anesthesia was maintained with 2% isoflurane in a mixture of 1 L/min of 100% oxygen. The tail vein was cannulated for intravenous access of MR contrast.

A transverse T2-weighted turbo spin echo sequence [repetition time (TR)/echo time (TE), 4930/128 msec; echo train length, 25; one signal acquired; matrix, 114×192] was performed with a section thickness of 1.0 mm, with an intersection gap of 0.12 mm and a flip angle of 160°. The field of view was 35×60 mm to cover the tumor completely (20 sections). T1 mapping was obtained using two variable flip angle acquisitions. Two precontrast T1 weighted measurements (3D VIBE; TR/TE, 8.32/2.29; matrix, 90×128) with different flip angles (2°, 15°) were performed with a section thickness of 1.04 mm (20 sections) and a field of view of 50×50 mm. This was followed by the dynamic contrast enhanced series using the TWIST sequence (TR/TE, 5.81/2.42; flip angle, 12°; other parameters were the same as the precontrast scan).

For the entire volume of 20 sections, the acquisition time was 6.2 seconds with a single signal acquired. This sequence was applied continuously for 60 measurements. After the first five measurements, an intravenous bolus injection of gadopentetate dimeglumine (Magnevist; Schering, Erlangen, Germany) at a concentration of 0.05 mmol/mL was administered manually at a dose of 0.3 mmol/kg over the maximum period of 5 seconds.

On completion of the study, data were transferred to an image processing workstation (Leonardo; Siemens Healthcare sector, Erlangen, Germany) and analyzed using Tissue 4D software (Siemens Healthcare sector, Erlangen, Germany). The dynamic data were fitted pixel by pixel to a pharmacokinetic model described by Tofts,[7,13] generating the transfer constant value, indicated by the symbol $K^{trans}$ (per second).

### Image analysis and measurement

Regions of interests were outlined on each MRI. Software generated values for $K^{trans}$, $K_{ep}$, and $V_e$ in each pixel and color maps for $K^{trans}$ pixel values. We selected values in the 95th percentile of distribution for each variable as being representative of quantitative parameters rather than the maximum, because the former was suggested to reduce motion induced errors, specifically in the periphery of a tumor.[14,15] We avoided mean values because they did not reflect the tumor heterogeneity, such as tumor necrosis. The largest length, width, and height of each tumor were measured from the T2-weighted images. Tumor volume was calculated by the formula of ellipsoid volume as follows:

$\pi/6\times L\times W\times H$[16]

Where L was length, W was width, and H was the height of the tumor, respectively.

To evaluate the changes in the values of $K^{trans}$ and tumor volume in the early radiation therapy periods, we defined ratios of $K^{trans}$, volume, and standard deviation as follows:

$K_1R=K_1/K_0$

$V_1R=V_1/V_0$

$SD_1R=SD_1/SD_0$,

Where $K_0$ values were of the 95th percentile of baseline $K^{trans}$, $V_0$ was the pretreatment tumor volume, and $SD_0$ was the standard deviation of $K^{trans}$ at baseline. $K_1$, $V_1$, and $SD_1$ were values taken after the first radiation therapy.

### Histological analysis

After performing DCE-MRI, the tumor was surgically excised from the right hind limb of the mice under ether anesthesia. The excised tumor was fixed with 10% formaldehyde solution and sliced in the transverse plane in 6 μm-thick slide sections, corresponding to the MR images. Histological analysis of the tumor was performed with hematoxylin and eosin staining to identify tumor necrosis and to evaluate tumor responses. Histological slides were scanned with a digital virtual microscope (Dotslide, Olympus, Hamburg, Germany). The outer tumor border and tumor necrosis were manually circumscribed using Image J software (NIH, Bethesda, MD, USA). Then the total pixel area of both the whole tumor and the necrotic region was automatically calculated. Histological necrotic fraction (NF) was defined by dividing the total pixel area of necrosis by the total pixel area within the tumor border. A "good response" was classified for tumors exhibiting a NF greater than 0.4.[17]

## RESULTS

Serial changes in the 95th percentile values for $K^{trans}$, $K_{ep}$, $V_e$, and tumor volume during radiation therapy were summarized in Table 1. While tumors with an NF of less than 0.4 were classified as demonstrating a poor response, mouse 3 with an NF of 0.49 was exceptionally classified as demonstrating a poor response, because a separate adjacent tumor had continuously grown after the first radiation ther-

**Table 1.** Sequential Changes in Quantitative DCE MRI Parameters during the Radiation Therapy

| No. | $K^{trans}$ ($sec^{-1}$) | | | | | | $K_{ep}$ ($sec^{-1}$) | | | | $V_e$ | | | | Tumor volume ($mm^3$) | | | | | | |
|---|---|---|---|---|---|---|---|---|---|---|---|---|---|---|---|---|---|---|---|---|---|
| | Baseline | RT | | | $K_1R$ | $SD_1R$ | Baseline | RT | | | Baseline | RT | | | Baseline | RT | | | $V_1R$ | NF | Response |
| | | 1st | 2nd | 3rd | | | | 1st | 2nd | 3rd | | 1st | 2nd | 3rd | | 1st | 2nd | 3rd | | | |
| 1 | 0.26 | 0.09 | 0.02 | 0.11 | 0.35 | 0.44 | 0.89 | 10.5 | 2.26 | 3.53 | 0.61 | 0.55 | 0.14 | 0.65 | 1183 | 2048 | 2160 | 2618 | 1.73 | 0.51 | G |
| 2 | 0.29 | 0.14 | 0.13 | 0.13 | 0.48 | 0.56 | 0.61 | 0.38 | 0.37 | 0.55 | 0.81 | 0.71 | 0.70 | 0.57 | 594 | 792 | 1020 | 1400 | 1.33 | 0.46 | G |
| 3 | 0.11 | 0.17 | 0.22 | 0.16 | 1.50 | 2 | 0.77 | 0.41 | 0.74 | 0.89 | 0.55 | 0.79 | 0.80 | 0.61 | 270 | 576 | 832 | 1224 | 2.13 | 0.49 | P* |
| 4 | 0.05 | 0.12 | 0.16 | 0.05 | 2.32 | 2 | 3.04 | 0.51 | 0.59 | 5.81 | 0.42 | 0.57 | 0.66 | 0.37 | 1176 | 1360 | 2167 | 3240 | 1.15 | 0.38 | P |
| 5 | 0.08 | 0.02 | 0.13 | 0.21 | 0.25 | 0.33 | 1.67 | 6.20 | 1.64 | 4.32 | 0.70 | 0.06 | 0.74 | 0.67 | 72 | 200 | 507 | 539 | 2.78 | 0.24 | P |

RT, radiation therapy; DCE-MRI, dynamic contrast-enhanced magnetic resonance imaging.
$K_1R$: ratio of $K^{trans}$; $SD_1R$: ratio of the standard deviation of $K^{trans}$; $V_1R$: ratio of the tumor volume after 1st radiation therapy to the baseline value, respectively.
NF (necrosis factor) is defined by dividing the total pixel area of necrosis by the total pixel area within the tumor border.
G: good response, NF>0.4; P: poor response, NF≤4.
*Exceptionally assigned to the poor response group due to adjacent outgrowth of tumor.

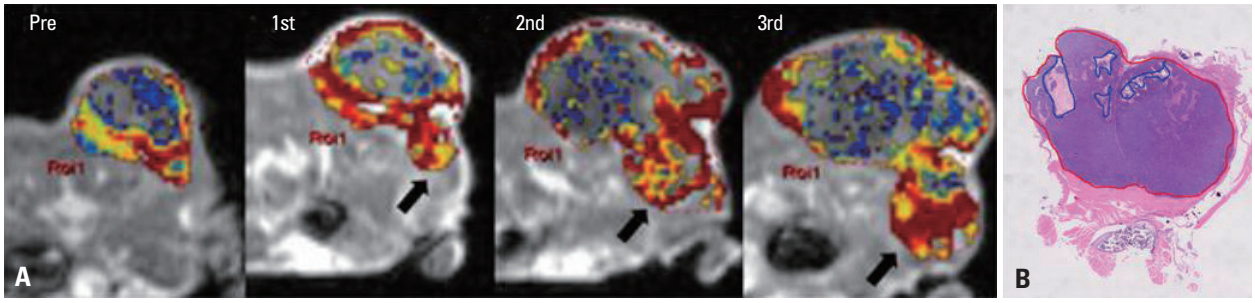


**Fig. 1.** An exceptional case, mouse #3, was assigned to the poor response group although it showed a large area of necrosis (NF=0.49). (A) Serial DCE-MRI with color mapping shows the change in $K^{trans}$. Pretreatment $K^{trans}$ showed a relatively low value (0.11). $K^{trans}$ increased after the first radiation therapy ($K_1R$=1.51). Red color represents the higher value of $K^{trans}$ and blue color represents the lower value. An outgrowing tumor was identified after the first radiation therapy (arrow). (B) H&E staining of the newly grown tumor, which separated from the main mass, showed rare necrosis. The original magnification is ×2. The red line indicates the tumor border and the blue line indicates the area of necrosis. NF, necrotic fraction; H&E, hematoxylin and eosin.

apy (Fig. 1).

The good response group (mice #1, 2) showed higher pretreatment $K^{trans}$ than the poor response group (mice #3, 4, 5). Two of the three mice in the poor response group (mice #4, 5) showed higher pretreatment $K_{ep}$ than those in the good response group (3.04, 1.67 vs. 0.89, 0.61). Two of the three mice in the poor response group (mice #3, 4) showed lower pretreatment $V_e$ than those in the good response group (0.55, 0.42 vs. 0.61, 0.81). Two of the three mice in the poor response group (mice #3, 5) showed lower pretreatment volume than those in the good response group (270, 72 vs. 594, 1183) (Fig. 2). All the mice in the good response group showed marked reductions in $K^{trans}$ and SD value after the first radiation. Two of the three mice (mice #3, 4) in the poor response group showed increased $K^{trans}$ ($K_1R$=1.50, 2.32 for mice #3, 4) and SD value ($SD_1R$=2 for both mice) after the first radiation therapy (Fig. 3). All tumors showed increased volume after the first radiation therapy. However, two of the three mice in the poor response group (mice #3, 5) showed greater volume increments than those in the good response group ($V_1R$=2.13, 2.78 for #3, 5 vs. 1.73, 1.33 for #1, 2).

## DISCUSSION

Over the past few years, CCRT or radiation therapy has been increasingly used to treat malignant neoplasms including rectal cancer.[18] Tumor vascularity and oxygenation status have long been advocated as important factors that influence tumor responses to radiation therapy.[5] DCE-MRI combined with pharmacokinetic modeling has emerged as a promising noninvasive imaging technique for evaluating tumor microvasculature.[6] Accordingly, previous studies suggested several DCE-MRI parameters for which to predict responses to radiation therapy in rectal cancer as well as other tumors. The most representative DCE-MRI derived parameter is the transfer constant, $K^{trans}$. However, the DCE-MR derived parameter $K^{trans}$ is still controversial as a biomarker for which to evaluate radiation therapy. de Vries, et al.[19] reported that high initial perfusion index (PI) value correlated with greater node down staging for radiation therapy in rectal tumor.[8] Meanwhile, Sahani, et al.[20] reported that initial high blood flow (BF) was negatively correlated with radiation therapy responses. They obtained BF as the representative parame-

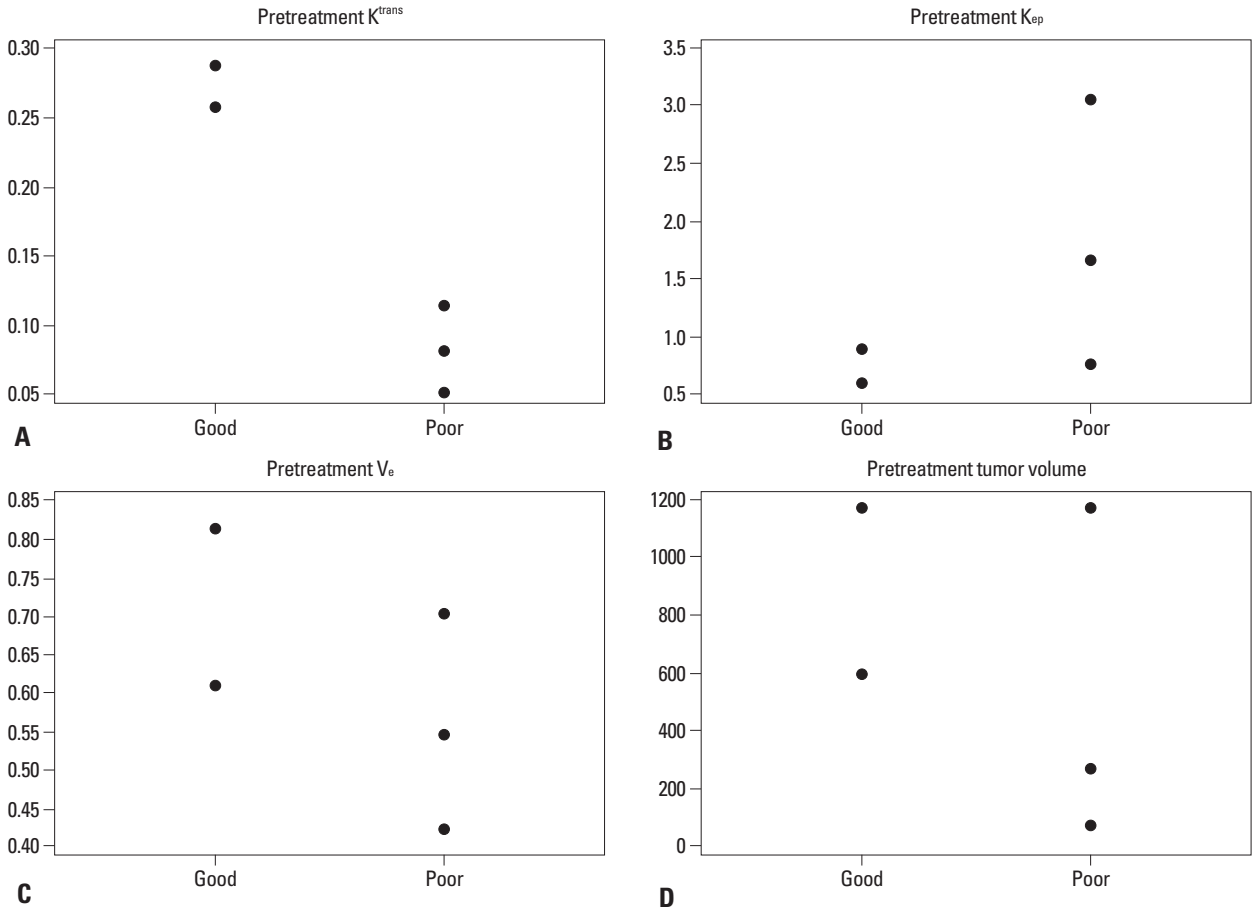


**Fig. 2.** Comparison of quantitative parameters between the good and the poor response groups upon baseline imaging. (A) $K^{trans}$, (B) $K_{ep}$, (C) $V_e$, (D) pretreatment tumor volume.

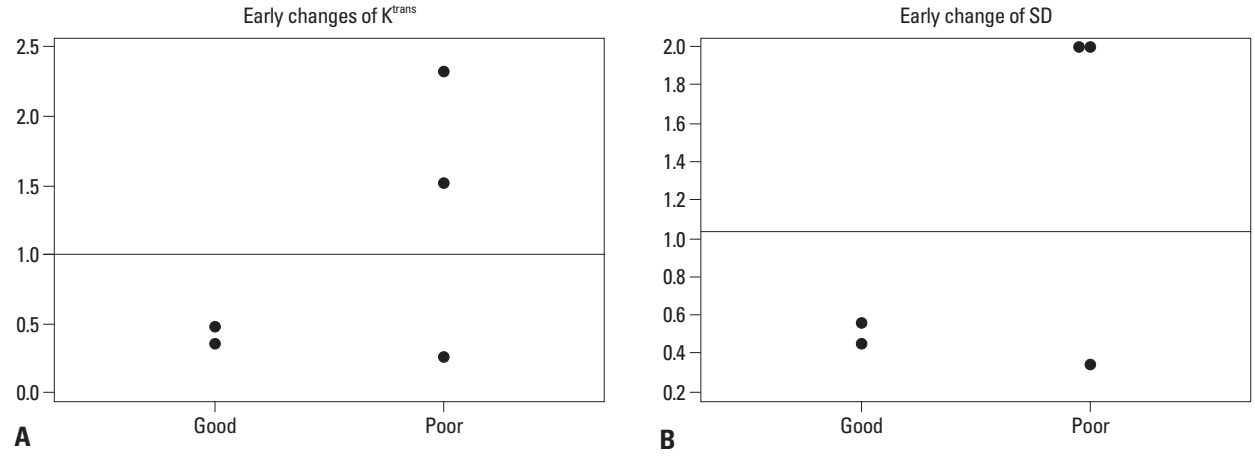


**Fig. 3.** Comparison of $K^{trans}$ between the good and the poor response groups after the 1st radiation therapy. (A) Early changes in $K^{trans}$ and (B) early changes in standard deviation for $K^{trans}$ (SD). The y-axis represents the ratio of the value after the 1st radiation therapy to the pretreatment value. The horizontal solid line at the ratio of 1 represents no change within the interval.

ter for their model using perfusion CT technique with the Johnson and Wilson model during 45 seconds of scan time. While De Vries, et al.[19] obtained PI value, which was shown to be associated with contrast extraction fraction as well as with perfusion using T1 dynamic contrast enhanced MRI technique with semi-quantitative analysis over 4 minutes. Different types of imaging modalities, mathematic models, scan times, and post processing methods might explain the previous inconsistent results. Although our results showed that the responder group had a marked higher $K^{trans}$ value at baseline scanning, the results should be carefully interpreted because our sample size was too small and we

used dynamic contrast enhanced MRI with Tofts two compartment model over one minute. Our results might support the hypothesis that the permeable vasculature may provide better oxygenation and showed efficient radiation sensitivity.[22] In addition, the good response to treatment group tended to exhibit lower $K_{ep}$ and higher $V_e$. Some studies reported that the initial values of $K_{ep}$ and $V_e$ might predict responses to radiation therapy.[23-25] However, their use remains highly debated and is not yet wholly established. Although $K_{ep}$ also reflects vessel density, perfusion, and permeability, it proved to be not as sensitive to tumor oxygenation as $K^{trans}$ in this study. However, $K_{ep}$ may have been confounded by interstitial volume fraction ($V_e$) in the necrotic area.[7]

Early reductions in $K^{trans}$ among good responders are in agreement with previous studies,[8,26] potentially indicating loss of immature tumor vessels. The good responders also showed early reductions in SD of $K^{trans}$, demonstrating a more homogenous distribution. Distributions of variables, such as SD, add further information for which to distinguish malignancy from benign disease to improve diagnostic accuracy.[11] Change in histogram heterogeneity has been reported in patients with rectal cancer after radiation therapy.[27] Changes in tumor size were also previously suggested as a strong predictor of responses.[10] In this study, good responders tended to show smaller volume increments than poor responders. However, tumor size change is not a perfect method for assessing the response of a tumor to treatment, as edema and necrosis refrain from measuring the exact tumor burden. For example, although mice #2 showed a good response and marked reduction in $K^{trans}$, tumor size masked the real tumor burden due to internal necrosis (Fig. 4).

This study has several limitations. First, fractionated doses of radiation therapy and intervals between the fractionated doses might not be optimized to suppress endothelial cell proliferation. Second, though CCRT is widely used in the treatment of advanced colorectal cancer, our results were limited to radiation therapy.

In summary, the good response to radiation therapy group in a DLD-1 colon cancer xenograft mouse model exhibited higher pretreatment $K^{trans}$ and early reductions in $K^{trans}$. Also, the distribution pattern of $K^{trans}$ in the early period of radia-

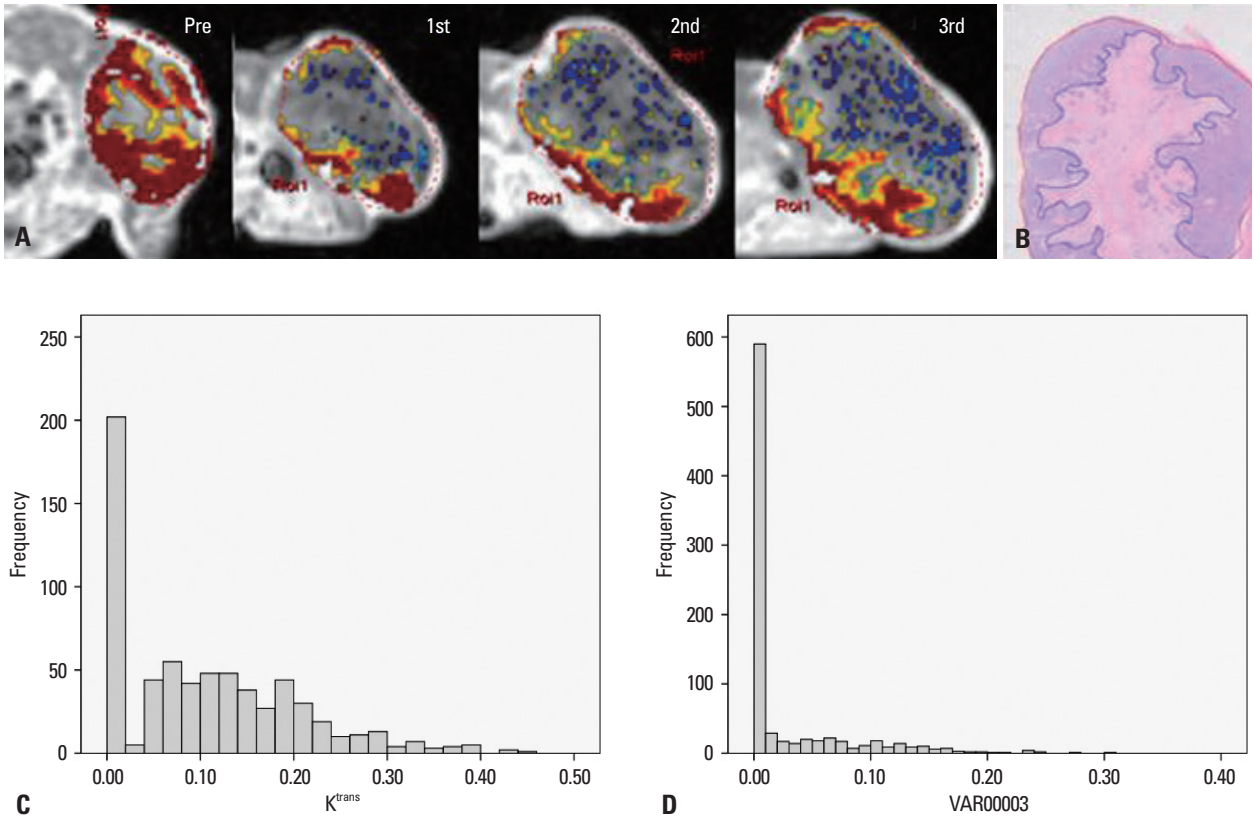


**Fig. 4.** A representative case of good response in mouse #2. (A) Serial DCE-MRI with color mapping shows higher pretreatment $K^{trans}$ (0.29) and marked reduction in $K^{trans}$ after the first radiation therapy ($K_1R$=0.47). (B) H&E staining of the corresponding section in mouse #2. The original magnification is ×2. Necrosis is identified in the center of the tumor. The red line indicates the tumor border and the blue line indicates the area of necrosis. The necrosis factor was 0.46. Histogram shows the heterogeneous distribution of $K^{trans}$ at baseline with an SD of 0.09 (C) and the homogenous distribution of $K^{trans}$ with an SD of 0.05 after the first radiation therapy (D). DCE-MRI, dynamic contrast-enhanced magnetic resonance imaging; SD, standard deviation; H&E, hematoxylin and eosin.

tion therapy became more homogenous.

## ACKNOWLEDGEMENTS

This study was supported by a grant from the Korean Health Technology R&D Project, Ministry of Health & Welfare, Republic of Korea (A110035). We would also like to acknowledge Siemens Healthcare Korea for their technical support as part of a cooperative research and development agreement.

## REFERENCES

1. Lindmark G, Gerdin B, Påhlman L, Bergström R, Glimelius B. Prognostic predictors in colorectal cancer. Dis Colon Rectum 1994;37:1219-27.
2. Marsh PJ, James RD, Schofield PF. Adjuvant preoperative radiotherapy for locally advanced rectal carcinoma. Results of a prospective, randomized trial. Dis Colon Rectum 1994;37:1205-14.
3. Sauer R, Becker H, Hohenberger W, Rödel C, Wittekind C, Fietkau R, et al. Preoperative versus postoperative chemoradiotherapy for rectal cancer. N Engl J Med 2004;351:1731-40.
4. Påhlman L, Glimelius B. The value of adjuvant radio(chemo)therapy for rectal cancer. Eur J Cancer 1995;31A:1347-50.
5. Harrison LB, Chadha M, Hill RJ, Hu K, Shasha D. Impact of tumor hypoxia and anemia on radiation therapy outcomes. Oncologist 2002;7:492-508.
6. McDonald DM, Choyke PL. Imaging of angiogenesis: from microscope to clinic. Nat Med 2003;9:713-25.
7. Tofts PS, Brix G, Buckley DL, Evelhoch JL, Henderson E, Knopp MV, et al. Estimating kinetic parameters from dynamic contrast-enhanced T(1)-weighted MRI of a diffusable tracer: standardized quantities and symbols. J Magn Reson Imaging 1999;10:223-32.
8. George ML, Dzik-Jurasz AS, Padhani AR, Brown G, Tait DM, Eccles SA, et al. Non-invasive methods of assessing angiogenesis and their value in predicting response to treatment in colorectal cancer. Br J Surg 2001;88:1628-36.
9. Ah-See ML, Makris A, Taylor NJ, Harrison M, Richman PI, Burcombe RJ, et al. Early changes in functional dynamic magnetic resonance imaging predict for pathologic response to neoadjuvant chemotherapy in primary breast cancer. Clin Cancer Res 2008;14:6580-9.
10. Yu HJ, Chen JH, Mehta RS, Nalcioglu O, Su MY. MRI measurements of tumor size and pharmacokinetic parameters as early predictors of response in breast cancer patients undergoing neoadjuvant anthracycline chemotherapy. J Magn Reson Imaging 2007;26:615-23.
11. Issa B, Buckley DL, Turnbull LW. Heterogeneity analysis of Gd-DTPA uptake: improvement in breast lesion differentiation. J Comput Assist Tomogr 1999;23:615-21.
12. Chang YC, Huang CS, Liu YJ, Chen JH, Lu YS, Tseng WY. Angiogenic response of locally advanced breast cancer to neoadjuvant chemotherapy evaluated with parametric histogram from dynamic contrast-enhanced MRI. Phys Med Biol 2004;49:3593-602.
13. Tofts PS. Modeling tracer kinetics in dynamic Gd-DTPA MR imaging. J Magn Reson Imaging 1997;7:91-101.
14. Jackson A, O'Connor JP, Parker GJ, Jayson GC. Imaging tumor vascular heterogeneity and angiogenesis using dynamic contrast-enhanced magnetic resonance imaging. Clin Cancer Res 2007;13:3449-59.
15. Patankar TF, Haroon HA, Mills SJ, Balériaux D, Buckley DL, Parker GJ, et al. Is volume transfer coefficient (K(trans)) related to histologic grade in human gliomas? AJNR Am J Neuroradiol 2005;26:2455-65.
16. Tomayko MM, Reynolds CP. Determination of subcutaneous tumor size in athymic (nude) mice. Cancer Chemother Pharmacol 1989;24:148-54.
17. Ahn SJ, An CS, Koom WS, Song HT, Suh JS. Correlations of 3T DCE-MRI quantitative parameters with microvessel density in a human-colorectal-cancer xenograft mouse model. Korean J Radiol 2011;12:722-30.
18. Rich TA, Skibber JM, Ajani JA, Buchholz DJ, Cleary KR, Dubrow RA, et al. Preoperative infusional chemoradiation therapy for stage T3 rectal cancer. Int J Radiat Oncol Biol Phys 1995;32:1025-9.
19. de Vries A, Griebel J, Kremser C, Judmaier W, Gneiting T, Debbage P, et al. Monitoring of tumor microcirculation during fractionated radiation therapy in patients with rectal carcinoma: preliminary results and implications for therapy. Radiology 2000;217:385-91.
20. Sahani DV, Kalva SP, Hamberg LM, Hahn PF, Willett CG, Saini S, et al. Assessing tumor perfusion and treatment response in rectal cancer with multisection CT: initial observations. Radiology 2005;234:785-92.
21. Choi S, Liu H, Shin TB, Lee JH, Yoon SK, Oh JY, et al. Perfusion imaging of the brain using Z-score and dynamic images obtained by subtracting images from before and after contrast injection. Korean J Radiol 2004;5:143-8.
22. Cooper RA, Carrington BM, Loncaster JA, Todd SM, Davidson SE, Logue JP, et al. Tumour oxygenation levels correlate with dynamic contrast-enhanced magnetic resonance imaging parameters in carcinoma of the cervix. Radiother Oncol 2000;57:53-9.
23. Loncaster JA, Carrington BM, Sykes JR, Jones AP, Todd SM, Cooper R, et al. Prediction of radiotherapy outcome using dynamic contrast enhanced MRI of carcinoma of the cervix. Int J Radiat Oncol Biol Phys 2002;54:759-67.
24. Hawighorst H, Knopp MV, Debus J, Hoffmann U, Grandy M, Griebel J, et al. Pharmacokinetic MRI for assessment of malignant glioma response to stereotactic radiotherapy: initial results. J Magn Reson Imaging 1998;8:783-8.
25. Pickles MD, Lowry M, Manton DJ, Gibbs P, Turnbull LW. Role of dynamic contrast enhanced MRI in monitoring early response of locally advanced breast cancer to neoadjuvant chemotherapy. Breast Cancer Res Treat 2005;91:1-10.
26. Hayes C, Padhani AR, Leach MO. Assessing changes in tumour vascular function using dynamic contrast-enhanced magnetic resonance imaging. NMR Biomed 2002;15:154-63.
27. de Lussanet QG, Backes WH, Griffioen AW, Padhani AR, Baeten CI, van Baardwijk A, et al. Dynamic contrast-enhanced magnetic resonance imaging of radiation therapy-induced microcirculation changes in rectal cancer. Int J Radiat Oncol Biol Phys 2005;63:1309-15.